Estimating Evapotranspiration with Land Data Assimilation Systems

C. D. Peters-Lidard[*1], S. V. Kumar[2,1], D. M. Mocko[2,1], and Y. Tian[3,1]

[1*]*NASA, Goddard Space Flight Center, Hydrological Sciences Branch, Code 614.3, Greenbelt, MD*

[2]*Science Applications International Corporation, Beltsville, MD*

[3]*Earth System Science Interdisciplinary Center, College Park, MD.*

Submitted to SPECIAL ANNUAL REVIEW ISSUE OF HYDROLOGICAL PROCESSES
July 2011, Revised October 2011

[*] Corresponding Author: Dr. Christa D. Peters-Lidard, NASA/Goddard Space Flight Center, Hydrological Sciences Branch, Code 614.3, Greenbelt, MD 20771 Phone: 301-614-5811; Fax: 301-614-5808; E-mail: christa.peters@nasa.gov; URL: http://lis.gsfc.nasa.gov.

Abstract

Advancements in both land surface models (LSM) and land surface data assimilation, especially over the last decade, have substantially advanced the ability of land data assimilation systems (LDAS) to estimate evapotranspiration (ET). This article provides a historical perspective on international LSM intercomparison efforts and the development of LDAS systems, both of which have improved LSM ET skill. In addition, an assessment of ET estimates for current LDAS systems is provided along with current research that demonstrates improvement in LSM ET estimates due to assimilating satellite-based soil moisture products. Using the Ensemble Kalman Filter in the Land Information System, we assimilate both NASA and Land Parameter Retrieval Model (LPRM) soil moisture products into the Noah LSM Version 3.2 with the North American LDAS phase 2 (NLDAS-2) forcing to mimic the NLDAS-2 configuration. Through comparisons with two global reference ET products, one based on interpolated flux tower data and one from a new satellite ET algorithm, over the NLDAS2 domain, we demonstrate improvement in ET estimates only when assimilating the LPRM soil moisture product.

Keywords

Land surface modeling, land data assimilation systems, evapotranspiration, soil moisture assimilation

INTRODUCTION

Land surface models predict terrestrial water, energy, momentum, and in some cases, biogeochemical exchange processes by solving the governing equations of the soil-vegetation-snowpack medium based on atmospheric boundary conditions including precipitation, radiation, wind, temperature, humidity and pressure. By constraining land surface models with observed atmospheric boundary conditions and land surface states, land surface data assimilation improves our ability to understand and predict terrestrial water and energy fluxes and states, including evapotranspiration. The ability to predict evapotranspiration is critical for applications in weather and climate prediction, agricultural forecasting, water resources management, and hazard mitigation (e.g., NRC, 2010; 2011). Until recently, global or continental land surface modeling at horizontal scales of 1 km or finer was infeasible due to limits in computational and observational resources.

Land Data Assimilation Systems (LDAS, Figure 1), are typically run "uncoupled" (or "offline") to estimate water and energy fluxes and states using observationally-based precipitation, radiation and meteorological inputs. However, they may also be run "coupled" to an atmospheric model for weather forecasts.

This paper reviews current and developing capabilities for estimating evapotranspiration (ET) using land surface models (LSMs) as part of an LDAS. First, we present a survey of land surface modeling for ET estimation, including recent intercomparison studies and LDAS efforts. Next, we compare LSM ET estimates from current LDAS systems to global gridded tower-based and remote sensing-based flux estimates. Finally, we present the results from simulations that

employ data assimilation (DA) of remotely sensed soil moisture measurements to improve LSM ET estimates.

BACKGROUND

The ability of LSMs or soil-vegetation-atmosphere transfer schemes (SVATS) to predict evapotranspiration has advanced significantly since the original bucket (Manabe, 1969), Simple Biosphere (SiB; Sellers et al., 1986) and Biosphere-Atmosphere Transfer Scheme (BATS; Dickinson et al., 1986) models pioneered at the National Oceanic and Atmospheric Administration's Geophysical Fluid Dynamics Laboratory (NOAA/GFDL), National Aeronautics and Space Administration's Goddard Space Flight Center (NASA/GSFC) and the National Center for Atmospheric Research (NCAR), respectively. Numerous advancements in second-generation LSMs have brought additional focus to snow physics and hydrology, such as the community Noah (Ek et al., 2003; Barlage et al., 2010; Livneh et al., 2010) and the Variable Infiltration Capacity (VIC; Liang et al., 1996; Bowling and Lettenmaier, 2010). So-called "third generation" LSMs include dynamic phenology and carbon stores, such as the Community Land Model (CLM; Bonan et al., 2002; Lawrence et al., 2011). To a large extent, this advancement has come as the result of three key community activities: first, the Global Land Atmosphere System Study (GLASS) intercomparison studies, second, the North American and Global LDAS projects, and third, the recent LandFlux initiatives. Below, we provide background on these efforts, including their major findings related to evapotranspiration estimation from LSMs.

GLASS Intercomparison Studies: PILPS, Rhone-AGG, and GSWP

The international GLASS panel, as part of the Global Energy and Water Cycle Experiment (GEWEX), has spearheaded three major intercomparison projects designed to evaluate the skill

of land surface models for predicting water and energy fluxes and states. The first was the Project to Intercompare Land-Surface Parameterization Schemes (PILPS; Henderson-Sellers et al., 1995; Pitman and Henderson-Sellers 1998). This project focused on a series of evaluations conducted in phases using specified atmospheric boundary conditions and parameters at points or regions. One of the key findings in this project is the documentation of the systematic improvements in LSMs from first-generation (bucket) to second-generation (e.g., SiB, BATS, Noah, VIC) through third generation (e.g., CLM). Another major finding from PILPS is the synthesis work by Koster and Milly (1997), in which it was shown that the interplay between the evaporation and runoff formulations in any LSM, could be expressed via two model-independent quantities: 1) the soil-depth-integrated evaporation sink efficiency and 2) the runoff-generation fraction over this integrated evaporation sink. A third major finding was that hydrologically-oriented models such as VIC were shown to be more skillful for continental scale water budgets.

The second major GLASS intercomparison projects, which represented a global-scale follow-on to PILPS, were the Global Soil Wetness Projects (GSWPs, Dirmeyer, 2011). GSWP-1 (Dirmeyer et. al, 1999) focused on the International Satellite Land-Surface Climatology Project (ISLSCP) Initiative I forcing data for the period 1987-88, and produced the first ever global, offline, multimodel land analysis based on “best possible” meteorological forcings. In addition, GSWP-1 served as a pathfinder for the NLDAS and GLDAS efforts described below. GSWP-2 (Dirmeyer et al., 2006) built on the foundation of GSWP-1, and produced 1 degree global multi-model fluxes and states for the ISLSCP II period from 1986-95 and showed that, in the absence of robust in-situ and/or remotely sensed soil moisture to provide constraints, the best estimate of soil wetness from multiple model products is a simple average. In addition to this finding,

GSWP-2 also derived multi-model soil wetness values normalized to the LSM dynamic range controlling the ET-runoff interplay, as described above in the PILPS analyses by Koster and Milly (1997). With respect to ET, GSWP-2 showed that ET has the smallest interannual variability of any water budget variable, and that global average transpiration is about one-third larger than direct evaporation from the soil. For the GSWP-2 period, latent heat flux exceeded sensible heat flux by about 20%, although that may reflect an absence of soil moisture limitations in later periods as observed by Jung et al. (2010) and discussed further below.

The third major intercomparison project, which occurred between GSWP-1 and GSWP-2, is known as Rhone-AGG (Boone et al., 2004). Rhone-AGG significantly advanced the community's ability to observationally diagnose deficiencies in LSM hydrological cycles by looking at spatial scaling of water and energy balance processes finer than GSWP (8km vs. 1^{o}), particularly the interplay of high-elevation snow accumulation/melt and lower-elevation streamflow. Techniques for evaluating and diagnosing physical processes with simulated hydrographs helped advance LSM's ability to simulate the daily hydrological cycles at multiple scales, most notably by implementing subgrid runoff formulations and elevation-based tiling for snow pack modeling. Rhone-AGG and GSWP-2 occurred in parallel with and greatly benefitted the development of NLDAS and GLDAS, as described in the following sections.

The North American Land Data Assimilation System

The primary goal of the North American Land Data Assimilation System (NLDAS; Mitchell et al., 2004; http://ldas.gsfc.nasa.gov/nldas/; http://www.emc.ncep.noaa.gov/mmb/nldas/) is to construct quality-controlled, and spatially- and temporally-consistent, land-surface model (LSM) datasets from the best available observations and model outputs. NLDAS is a collaboration project among several groups: NOAA/NCEP's Environmental Modeling Center (EMC), NASA's

Goddard Space Flight Center (GSFC), Princeton University, the University of Washington, the NOAA/NWS Office of Hydrological Development (OHD), and the NOAA/NCEP Climate Prediction Center (CPC). The NLDAS project produces a LSM forcing dataset from a daily gauge-based precipitation analysis (temporally disaggregated using hourly radar data, satellite estimates, or other sources), bias-corrected shortwave radiation, and surface meteorology reanalyses. This forcing is used to drive four separate LSMs to generate hourly model outputs of surface fluxes, soil moisture, snow cover, and runoff. The current operational version of NLDAS uses the following LSMs: Noah – from NOAA/NCEP, Mosaic – from GSFC, VIC – from Princeton University, and SAC – from NOAA/OHD. Datasets and simulations from NLDAS Phase 2 (NLDAS-2) extend back to January 1979 and continue to be produced in near real-time on a 1/8th-degree grid over central North America (from 25 to 53N and 125 to 67W). NLDAS individual and ensemble-mean LSMs are also used for drought monitoring and as part of an experimental drought forecast system. The ensemble-mean on the drought monitor is a simple type of a multi-model analysis of LSMs, which have been shown to improve the depiction of simulated states in many ways (e.g., Guo et al., 2007, for GSWP-2 datasets). NLDAS data products are distributed at EMC as well as at the NASA Goddard Earth Sciences Data and Information Services Center (GES DISC; http://disc.gsfc.nasa.gov/hydrology/).

The first incarnation of the project, Phase 1 (NLDAS-1), comprised data since October 1996 and consisted of a somewhat-similar yet different LSM forcing dataset (Cosgrove et al., 2003). Earlier versions of the same four LSMs (Noah, SAC, VIC, and Mosaic) were used in NLDAS-1 as well. NLDAS-1 datasets were extensively evaluated and validated against available observations in numerous studies, including examinations of the forcing (Luo et al., 2003) and of

the LSM output (Robock et al., 2003). Robock et al. evaluated the LSM-simulated soil moistures and temperatures against observations from the Oklahoma Mesonet, and also evaluated surface latent, sensible, and ground fluxes using ARM/CART stations. They found that the Noah LSM was closest to the observations of the latent heat flux in this region over a two-year period. Lohmann et al. (2003) intercompared water balance and streamflow between the LSMs and found regional differences up to a factor of 4 in the simulated mean annual runoff and up to a factor of 2 in the mean annual evapotranspiration, with monthly differences even greater. Other land parameters evaluated from NLDAS-1 included soil moisture (Schaake et al., 2004), snow cover extent (Sheffield et al., 2003), and snow water equivalent (Pan et al., 2003). Many of these studies from NLDAS-1 also tested the effects of LSM physics and parameter changes on the evaluation results.

The NLDAS-2 forcing dataset corrects the daily gauge precipitation analysis using a PRISM (Parameter-elevation Regressions on Independent Slopes; Daly et al., 1994) method which considers the topographic effect on precipitation. The precipitation is temporally disaggregated to hourly, primarily using Stage II radar data. In locations/times when the radar data is not available, satellite retrievals, a coarser-scale hourly gauge analysis, or reanalysis data is used. The non-precipitation land-surface forcing fields for NLDAS-2 are derived from the analysis fields of the NCEP North American Regional Reanalysis (NARR, Mesinger et al., 2006). Surface pressure, surface downward longwave radiation, and near-surface temperature and humidity fields are vertically adjusted to the terrain on the NLDAS grid. The surface downward shortwave radiation is bias-corrected using GOES satellite observations. NLDAS-2 also contains numerous improvements to the equations of the LSMs as well as their calibration. The

141 snow physics in the Noah LSM was upgraded (Livneh et al., 2010), VIC model parameters were
142 calibrated using streamflow observations (Troy et al., 2008), SAC used an updated potential
143 evaporation dataset (Xia et al., 2011b), and Mosaic used updated model parameters (for details,
144 see Robock et al., 2003). Xia et al. (2011a) analyzed water and energy fluxes in the upgraded
145 NLDAS-2 LSMs, including their ensemble-mean and model spread. In a separate study, Xia et
146 al. (2011c) examined the spatial distribution of the correlation between monthly-mean
147 precipitation and evapotranspiration (ET) the four LSMs; they found that the two soil vegetation
148 atmosphere transfer (SVAT) LSMs (Noah and Mosaic) had a stronger correlation, while the two
149 hydrological LSMs (VIC and SAC) had a stronger correlation between the precipitation and
150 runoff. Wei et al. (2011) evaluated improvements of the Noah LSM related to warm season
151 simulation in NLDAS by adding a seasonally- and spatially-varying LAI as well as
152 modifications to Noah's treatment of the vertical profile of root density, the minimum stomatal
153 resistance parameters, the diurnal variation of surface albedo, the roughness length for heat, and
154 the vapor-pressure and soil moisture deficit terms. This study compared the NLDAS-2 version
155 of Noah to ARM/CART latent heat flux observations and found reduced biases, which also
156 helped improve the simulation of the mean annual water balance. Mo et al. (2011) compared ET
157 from three NLDAS-2 LSMs against Ameriflux observations and found that Noah and VIC
158 tended to exhibit low ET biases in the winter, with slight high ET biases in the summer, despite
159 no apparent biases in NLDAS-2 net radiation. Mosaic generally had higher ET than the
160 observations as well as from Noah and VIC, with a three-member ensemble-mean performing
161 the best,, consistent with the findings of GSWP discussed in the previous section. Kovalskyy et
162 al. (2011) estimated evapotranspiration using a scheme that combines a water balance model
163 with an event-driven phenology model, driven with NLDAS-2 forcing; they compared these

estimates against ET from the MODerate Resolution Imaging Spectroradiometer (MODIS) instrument (Mu et al., 2007) as well as from the NLDAS-2 Mosaic LSM, and showed better agreement to the MODIS-derived ET at the 5-km scale of the study.

The Global Land Data Assimilation System

The Global Land Data Assimilation System (GLDAS) led at NASA/GSFC (Rodell et al., 2004a) also uses satellite- and ground-based observations to construct a forcing dataset to drive four LSMs. The four LSMs in GLDAS are Noah, Mosaic, VIC, and CLM, and GLDAS data extends globally from January 1979 at both 1.0-degrees (all LSMs) and 0.25-degrees (Noah only). In addition to extending an NLDAS-style framework to the global scale, GLDAS was one of the first LDASs to routinely assimilate satellite-based surface states to improve simulated water and energy fluxes and states. GLDAS has included data assimilation of MODIS snow cover to constrain the modeled SWE (after Rodell and Houser, 2004), and has also studied the effects of assimilating remotely-sensed skin temperatures and soil moistures. While considering ET produced by GLDAS, Rodell et al. (2004b) compared basin-scale estimates of evapotranspiration produced by GLDAS/Noah and other models against a water balance approach using the Gravity Recovery And Climate Experiment (GRACE) satellites, and found that the GRACE estimates were generally within the range of the model results, and the biases were consistent and the uncertainty on the same order as GRACE.. Kato et al. (2007) examined the choice of LSM, land cover, soils, elevation, and forcings using GLDAS on the simulated latent and sensible heat fluxes and soil moisture compared to CEOP in situ observations. They found that the LSM choice had the biggest effect on the simulated output (including ET), and that ET was most sensitive first to precipitation, then land cover, and then radiation. Syed et al. (2008) compared variations in terrestrial water storage from GRACE compared to GLDAS

simulations and found that ET was most effective in dissipating terrestrial water storage in the mid-latitudes. Despite all these detailed studies, however, none have directly evaluated both GLDAS and NLDAS using observations over CONUS. One study that did compare early versions of both systems (Jambor et al.,2002) demonstrated the benefit of satellite-based precipitation used in conjunction with model precipitation in GLDAS while using the gauge-based precipitation in NLDAS as the evaluation dataset. Overall, GLDAS's advancements in land data assimilation and GRACE-based ET estimation significantly advanced the ability of LSMs to estimate ET, subject to observational constraints.

The LandFlux Initiative and Reference ET Products

The LandFlux initiative has been coordinated by the GEWEX Radiation Panel to develop and evaluate consistent and high-quality global ET datasets for climate studies. Recently developed capabilities for global ET estimation using LSMs (as discussed above) as well as techniques for synthesizing satellite data, flux tower data, and atmospheric reanalyses provide the opportunity to produce global ET products using different approaches. The LandFlux-EVAL project (Mueller et al., 2011; Jiménez et al., 2011) is currently evaluating multiple global ET products produced using four different categories of techniques: 1) Observations-based diagnostic datasets; 2) observationally-driven "offline" LSM products (e.g., GSWP, GLDAS); 3) atmospheric reanalyses; and 4) IPCC AR4 simulations from 11 GCMs. In Mueller et al., 41 global land ET datasets were evaluated along with IPCC AR4 GCM simulations for the 1989–1995 time period. An interesting finding of a cluster analysis conducted as part of this study is that the GLDAS-Noah and CLM products were closely related to two different reference ET products, including the Jung et al., 2009 product described further below.

Jiménez et al. (2011) evaluated 12 monthly mean land surface ET and other flux products for the period 1993–1995 and found that the 12-product global annual mean latent heat flux (Qle) was approximately 45 Wm^{-2} with a spread of approximately 20 Wm^{-2}. Similar spreads were found for sensible (Qh) and net radiative (Rn) fluxes, with larger spreads for tropical rainforest year-round and grassland or crop in the dry season. Analysis for large river basins indicated large spreads for the Danube, Congo, Volga, and Nile basins, with smaller spreads for other basins, including the Mississippi.

One of the key reference datasets for the LandFlux-EVAL effort, also used as one of the reference datasets in our LDAS analysis described in subsequent sections, is the Max Planck Institute (MPI) flux dataset from Jung et al., (2009), which was created by synthesizing FLUXNET (Baldocchi et al., 2001) tower data with meteorological forcings and vegetation information from interpolated station and satellite data to produce a global, monthly, 1/2 degree resolution estimate of land ET from 1982 to 2008. Jung et al. (2010) found that global annual ET has been increasing by approximately 7 mm per year per decade during the period 1982-1997, with moisture limitation eliminating this trend during the period 1998-2008. Another ET product used as a reference dataset in this study is the global 1km ET estimates based on MODIS satellite data (Mu et al., 2011). In this dataset, ET estimates are derived using Mu et al. (2011)'s algorithm, which is improved relative to the previous Mu et al. (2007) work. The ET algorithm is primarily based on the Penman-Monteith equation and considers the surface energy partitioning and environmental constraints to derive ET. In this study, we employ the monthly averaged MOD16 ET datasets.

Although the LandFlux-EVAL effort has compared model-based GLDAS and GSWP flux estimates to observationally-based MOD16 and MPI reference flux estimates, a key question not previously addressed by LandFlux-EVAL is the extent to which assimilating observed soil moisture can reduce the differences between the model-based and observationally-based flux estimates. Addressing this question is one of the primary motivations of the current work.

EXPERIMENTAL SETUP

To illustrate the current capability of the current LDAS systems to simulate evapotranspiration at continental scales, we compare estimates from GLDAS, and two NLDAS-equivalent simulations over the NLDAS-domain with two reference datasets: (1) the gridded FLUXNET dataset from Jung et al. (2009) and (2) the MOD16 dataset developed by Mu et al. (2011). Further, we also present estimates from the NLDAS-equivalent simulations that employ the assimilation of satellite surface soil moisture retrievals. Because the NLDAS uses only a single version of the Noah LSM, we chose to produce our NLDAS-equivalent products using the Land Information System (LIS; Kumar et al., 2006, Peters-Lidard et al., 2007) with Noah versions 2.7.1 and 3.2 so that we can examine the impacts of recent physics changes in Noah on ET estimation. The experiments employ the same domain configuration used in the NLDAS project (from 25-53^{o}N and 125-67^{o}W at 1/8th-degree resolution) and are designed in a manner as similar as possible to the NLDAS-2 Noah model simulations. While the forcings and NLDAS-equivalent simulations are at a 1/8 degree horizontal resolution, we average the outputs to ½ degree resolution prior to comparisons with the FLUXNET and MOD16 datasets. The GLDAS Noah datasets are similarly averaged from ¼-degree to the ½ degree resolution. The forcing for the NLDAS-equivalent runs is the NLDAS-2 described above. The simulations are run with a 15

minute timestep, and the models are spun up by running from 1979 to 1985 and then reinitializing the model from 1979 to generate outputs from 1979-2010.

In the data assimilation integrations, we employ surface soil moisture data derived from the Advanced Microwave Scanning Radiometer for the Earth Observing System (AMSR-E) sensor aboard the Aqua satellite. Two different AMSR-E retrieval products are employed in the data assimilation simulations; (1) the NASA Level-3, "AE_Land3" product (version 6, Njoku et al., 2003) and (2) AMSR-E Land Parameter Retrieval Model (LPRM) product developed at NASA GSFC and VU Amsterdam (Owe et al., 2008). The NASA product is primarily based on X-band brightness temperatures, whereas both X-band and C-band brightness temperature-based retrievals are used in the LPRM product. Measurements from both ascending and descending overpasses are used in these products. A number of quality control measures are applied to the soil moisture retrievals prior to data assimilation, similar to the approaches followed in Reichle et al. (2007) and Liu et al. (2011). In the soil moisture products, retrievals flagged for dense vegetation, precipitation, snow cover, frozen ground, and Radio Frequency Interference (RFI) are excluded in the assimilation system. Further, additional quality control is applied based on the information from the land surface model, where the retrievals are excluded when the land surface model indicated active precipitation, non-zero snow cover, frozen soil or dense vegetation (when green vegetation fraction > 0.7).

The assimilation integrations employ a one-dimensional Ensemble Kalman Filter (EnKF) algorithm, which is a widely used technique for soil moisture data assimilation (Reichle et al., 2002, Crow and Wood, 2003, Reichle et al., 2007, Kumar et al., 2008, Kumar et al., 2009). An

ensemble size of 12 is used in these simulations (Kumar et al., 2008), with perturbations applied to both the meteorological fields and model prognostic fields to simulate uncertainty in the soil moisture fields. The parameters used for these perturbations are listed in Table 1, which are based on earlier data assimilation studies (Kumar et al., 2009). As algorithms such as EnKF are designed to correct random, zero-mean errors and assume the use of unbiased observations relative to the model generated background, it is often a common practice to scale the observations prior to data assimilation to match the model's climatology (Reichle and Koster, 2004, Drusch et al., 2005, Reichle et al., 2007, Kumar et al., 2009). Here we employ the Cumulative Distribution Function (CDF)-scaling approach of Reichle and Koster (2004), where the observations (roughly corresponding to a maximum depth of 2cm) are rescaled to the model's 10cm surface soil moisture climatology by matching the CDF of the observations to the CDF of the model soil moisture. The model CDF and observation CDF are computed using 7 years of data (2002-2008), separately for each grid point.

As the soil moisture retrievals are available only from 2002 onwards, the NLDAS-equivalent simulations with data assimilation are conducted during the period of 2002-2008. During this period, we update not only the surface (10cm) soil moisture in Noah, but also the layer 2 through layer 4 soil moisture, following the parameters in Table 1. The comparisons presented in next section are limited to the data assimilation period (2002-2008).

CURRENT RESEARCH FINDINGS AND FUTURE WORK

The results presented in this section focus first on the evaluation of the LDAS ET estimates that do not employ data assimilation. This is followed by the description of the impact of soil moisture data assimilation on ET estimation.

Evaluation of the ET estimates from LDAS simulations

Table 2 presents the domain-averaged root mean square and bias errors and the associated 95% confidence intervals, for latent (Qle) and sensible (Qh) heat flux estimates from the three LDAS simulations compared against the gridded FLUXNET and MOD16 datasets. This table also shows results from the data assimilation experiments to be discussed in the next section. Overall, the NLDAS-like simulation using the Noah 2.7.1 model provides better estimates of Qle (RMSE of 19.3 Wm^{-2} against FLUXNET and 21.5 Wm^{-2} against MOD16) relative to other products. Average seasonal cycles of these error metrics stratified monthly are presented in Figure 2. In both sets of comparisons, the largest differences between the LDAS simulations are observed during the spring and fall months, with NLDAS-like simulations with Noah 2.7.1 providing the better estimates. Qle estimates from GLDAS show underestimation in the late summer and fall months and an overestimation in the spring and early summer months, relative to both reference datasets. Comparatively, NLDAS-like integration with Noah 2.7.1 indicates lower biases most months, but the biases are consistently positive. Though Noah 3.2 is a newer version of the Noah model, the flux estimates appear to be degraded overall relative to Noah 2.7.1, with the comparison against FLUXNET data indicating more severe degradations relative to the MOD16. This may reflect uncertainty in the reference flux datasets during the springtime, in particular. During the fall months, bias estimates in Noah 3.2 are improved relative to Noah 2.7.1 (in the comparisons against FLUXNET), but during spring and summer months, biases in Noah 3.2 ET increase compared to that of Noah 2.7.1. It can be noted that these trends in RMSE and bias errors are highly statistically significant, as indicated by the 95% confidence interval values given for each error estimate. Note that any spatial auto-correlation of RMSE and Bias values across the domain is ignored in computing these confidence intervals. The tight intervals

329 reported in Table 2 are likely to increase if allowances for spatial autocorrelation of errors are
330 included in the confidence interval computations. The trend of increased flux error estimates in
331 Noah 3.2 relative to Noah 2.7.1 is likely a result of the changes in model parameters (such as
332 LAI) along with other changes to Noah's warm season physics as described in Wei et al. (2011).
333 As discussed in the Background section, Wei et al. (2011) showed improvement of these physics
334 changes when compared to ARM/CART flux datasets, whereas our analysis uses gridded data
335 (FLUXNET and MOD16) over the entire NLDAS domain, including many different vegetation
336 types and climate regimes. Other studies (also presented in the Background section) showed
337 Noah 3.2's improved simulation of streamflow, snow, and other hydrologic variables relative to
338 Noah 2.7.1.
339
340 Figure 3 provides an intercomparison of the seasonally-averaged Qle computed using
341 estimates from three consecutive months (DJF represents December-January-February, MAM
342 represents March-April-May, JJA represents June-July-August and SON represents September-
343 October-November) from the three LDAS integrations and the two reference datasets, the
344 gridded FLUXNET and MOD16 product. Relative to FLUXNET, all three LDAS datasets show
345 higher ET in the spring MAM months in the Southeast and Lower Mississippi River Basin.
346 During JJA, however, GLDAS compares much better than the NLDAS-like Noah simulations.
347 Interestingly, the Noah 2.7.1 and Noah 3.2 results for JJA are generally similar except over
348 highly vegetated crop regions in the upper Midwest and the irrigated growing areas along the
349 Mississippi River. Neither reference dataset seems to reflect irrigated areas (see, for example
350 Table 4 in Mu et al., 2011), and the differences in Noah2.7.1 and Noah3.2 do not include
351 irrigation effects, so these differences for crops are likely due to changes in the aerodynamic

conductance formulation in Noah, implemented primarily for improved snowmelt modeling. Here, the Noah 3.2 JJA Qle is much higher, indicating that the parameter values used for the vegetation type(s) in these regions may need refinement. A closer look during MAM also shows this same pattern with higher Qle in Noah 3.2 relative to Noah 2.7.1. It can be noted that except MOD16, all other datasets show an artifact of lower Qle in California and West Coast regions. Interestingly, the higher Qle areas for MOD16 do not seem to correspond to known irrigated areas. During the fall SON months, the Qle from GLDAS is low compared to FLUXNET, particularly over the Upper Plains and Southeast; the Noah simulations show a pattern overall much closer to FLUXNET, but with too high Qle magnitudes right along the Gulf Coast. MOD16, on the other hand, indicates lower Qle over the High plains consistent with GLDAS, and higher Qle over the Southeast, consistent with the NLDAS-based estimates.

Impact of soil moisture data assimilation on ET estimates

Figure 4 provides a comparison of the average seasonal cycles of RMSE and Bias in Qle estimates (again, relative to the two reference datasets) from the NLDAS-like simulation without any data assimilation (termed as the "open loop" (OL) simulation) and the two integrations that employ the assimilation of surface soil moisture retrievals from NASA and LPRM products (NASA-DA and LPRM-DA, respectively). In this comparison, all three model integrations employ Noah 3.2. It can first be observed that the assimilation of soil moisture retrievals impact the Qle estimates, primarily during the summer and fall months. The Qle estimates from the open loop simulation are systematically improved by the assimilation of LPRM soil moisture retrievals, whereas the assimilation of NASA retrievals shows degradation. Compared to FLUXNET, the domain averaged RMSE of the open loop integration is 27.6 Wm^{-2} and it increases to 29.4 Wm^{-2} in the NASA-DA integration (Table 2). The improvements shown in

376 Figure 4 from LPRM-DA translates to a domain averaged RMSE of 25.6 Wm^{-2} when compared
377 to FLUXNET. The trends in RMSE and Bias are similar in the comparisons against MOD16.
378 The RMSE of the open loop integration is 22.7 Wm^{-2} and it improves to 21.9 Wm^{-2} with the
379 assimilation of LPRM soil moisture retrievals. The assimilation of NASA soil moisture retrievals
380 degrades the ET estimates, with a domain averaged RMSE of 24.5 Wm^{-2}.
381
382 To quantify the spatial improvements due to assimilation, we define an "improvement
383 metric" as difference between the RMSE of the integration with data assimilation and the RMSE
384 of the open loop integration (RMSE (DA) – RMSE (OL)). If data assimilation improves the flux
385 estimates (i.e., reduces the RMSE), then the improvement metric will be negative. On the other
386 hand, the improvement metric will be positive if the assimilation simulation degrades the flux
387 estimates. Figures 5 and 6 present a comparison of the improvement metric stratified seasonally,
388 from both assimilation integrations, as compared to both reference ET datasets. Figure 5
389 represents the improvement metric when using the NASA AMSR-E product and Figure 6 shows
390 the corresponding comparisons when using the LPRM product. In both sets of comparisons, the
391 LPRM-based assimilation provides more systematic improvements in the flux estimates, whereas
392 the NASA-based integration indicates degradations over several regions. For example, during
393 MAM months, the flux estimates from NASA-DA show degradation over the Southern Great
394 Plains, with improvements observed over Illinois, Indiana, Ohio and areas along the Mississippi
395 river; these are the same areas discussed earlier in Figure 3 where Noah 3.2 had higher simulated
396 ET. The LPRM-integration on the other hand, shows improvements over large areas of
397 Midwest, and South-central U.S during MAM, with no significant degradations observed as a
398 result of soil moisture assimilation. During JJA, the NASA-DA shows degradations in most

regions interspersed with improvements over a few regions near North Dakota, Illinois, Eastern Texas and the West coast, in the comparisons using the FLUXNET data. The MOD16-based comparisons show similar results, with small regions of improvements over the Central and Eastern US with degradations over most of the domain. In contrast, the JJA comparisons for LPRM-DA show degradations in a few regions only, with improvements observed over large areas of the Midwest U.S. During the SON months, similar trends are seen, with degradations over Mexico and regions near Ohio and Illinois (when compared to FLUXNET) and Mississippi river basin areas (when compared to MOD16). The LPRM-DA based simulations show improvements over Midwest and Central US in the comparisons against MOD16 and no significant degradations in the comparisons against FLUXNET.

Further analysis of the differences shown in Figures 5 and 6 reveals that the magnitudes of the differences are strongly related to landcover type. Based on further analysis (not shown), stratifying the Qle RMSE improvements due to DA with respect to landcover type, we found that the most significant improvements occur in croplands for both soil moisture datasets and both reference datasets. Grassland was also found to have significant changes in Qle RMSE with both datasets, and more so with respect to the MOD16 reference data. In general, DA does not occur over heavily vegetated regions, due to masking out high-vegetation water content areas which make soil moisture retrievals difficult. Nonetheless, our results suggest modest changes over evergreen needleleaf forests and woodlands, especially for the NASA product.

In order to relate the improvements and degradations in latent heat flux estimates to changes in soil moisture resulting from data assimilation, we present a comparison of the surface soil moisture difference maps in Figure 7. The difference maps represent the mean surface soil

422 moisture of the data assimilation integration subtracted by the mean surface soil moisture of the
423 open loop integration. In other words, the difference maps represent the changes in soil moisture
424 values introduced by data assimilation, averaged seasonally. A negative difference indicates that
425 the soil moisture is drier due to assimilation and a positive difference indicates that the soil
426 moisture is wetter from assimilation. By comparing Figures 5 and 6 against Figure 7, it can be
427 observed that the spatial patterns of the improvement metric correlates well with those of the soil
428 moisture difference maps. For example, during MAM, both the NASA-DA and the NASA-
429 LPRM (with a smaller magnitude) soil moisture difference maps indicate drier patterns over
430 Illinois, Indiana, Ohio and areas along the Mississippi river that leads to corresponding
431 improvements in latent flux estimates (Figure 5) over these same regions. During JJA, the soil
432 moisture changes due to assimilation of NASA and LPRM are generally of opposite sign, and
433 seem to show a mix of improvements and degradations in the fluxes, depending on landcover. .
434 During SON, assimilation of NASA retrievals dries the soil moisture over Lower Texas and
435 Mexico (relative to OL) and it leads to a corresponding degradation in the flux estimates over
436 these regions when compared to FLUXNET (Figure 5, panel for SON). Similar patterns of tight
437 correlation between the soil moisture difference patterns and the flux improvement patterns can
438 be observed in the LPRM-DA integration. During JJA, over the Midwest US, the LPRM-DA
439 causes the soil moisture simulations to be drier than the open loop simulation leading to
440 improvements in the latent heat flux estimates over the same areas.
441
442 It is important to note that the CDF-scaling approach for data assimilation used here (and
443 described previously) is intended to preserve the soil moisture climatology of the LSM, while
444 taking advantage of observed anomalies. Therefore, the results suggest that the

improvements/degradations in Qle due to soil moisture assimilation are a direct result of improved/degraded soil moisture stress responses in the stomatal resistance formulation of the Noah 3.2 LSM. This sort of non-linear feedback is likely due to the ability of LPRM-DA to redistribute water in a seasonal cycle that corresponds to Noah's biases in soil moisture and ET. By design, and verified by us (not shown) the soil moisture increments from both NASA-DA and LPRM-DA do not change the mean surface soil moisture relative to the open loop. However, as most easily explained via the bias time series in Figure 4, significant seasonal changes in soil moisture, translate into varying ET responses. In winter, the change in ET from the OL to the DA is nominal (since Rnet, and therefore Qle is small). In spring, LPRM tends to reduce soil moisture relative to the open loop and therefore Qle bias while NASA-DA increases soil moisture and Qle bias. In the summer, the open loop skill is higher, and both products further compensate for errors, with LPRM tending to overdry and NASA tending too wet. Overall, the net effect is a domain-averaged increase of 2 Wm^{-2} in total Qle for the LPRM-DA, and a 3 Wm^{-2} reduction in Qle for NASA-DA.

Evaluation of the surface energy partition from LDAS simulations

The surface energy partition consists of two key components, the latent heat and the sensible heat fluxes. Though the primary focus of this article is to evaluate the latent heat estimates, we also evaluated the sensible heat flux (Qh) estimates from the LDAS simulations using FLUXNET data to examine if the trends seen in the Qle estimates are consistent for both energy partition terms. Trends in error metrics similar to those seen with latent heat flux estimates are found in the sensible heat estimates. As shown in Table 2, Qh estimates from GLDAS has a domain averaged RMSE of 23.4 Wm^{-2} whereas the NLDAS-like simulations with Noah 2.7.1 and Noah 3.2 have domain averaged RMSEs of 21.1 and 32.5 Wm^{-2}, respectively. The

assimilation with LPRM data improves the domain averaged RMSE to 30.4 Wm^{-2} (over that of the open loop integration NLDAS-like simulation with Noah 3.2), whereas the assimilation of NASA retrievals degrades the sensible heat flux estimates with a domain averaged RMSE of 34.5 Wm^{-2}. Spatial patterns of improvements and degradations similar to that seen in Figures 5 and 6 are observed for sensible heat fluxes as well (not shown; for FLUXNET only, as Qh is not available from MOD16). Again, these trends are statistically significant, as seen from the confidence interval values presented in Table 2.

SUMMARY

This article provides a description of the capabilities of Land Data Assimilation Systems (LDAS) for generating ET estimates and presents a quantitative evaluation of ET estimates, expressed as latent heat flux (Qle), from a number of LDAS simulations. The simulated ET values from GLDAS and LSM simulations conducted over the NLDAS-domain using two different versions of the Noah land surface model (Noah version 2.7.1 and version 3.2) are compared against two reference ET datasets: the gridded tower-based estimates from the FLUXNET measurements and ET estimates based on MODIS satellite data, known as the MOD16 product. The article also presents an evaluation of the impact of soil moisture data assimilation in ET estimation. The data assimilation integrations employ two different retrievals of the AMSR-E soil moisture measurements; the NASA Level-3 product and the AMSR-E Land Parameter Retrieval Model product from VU Amsterdam.

The evaluation of ET fields indicate that the simulation using NLDAS forcing with Noah 2.7.1 provides slightly better estimates among the LDAS simulations without data assimilation, although all Noah simulations suffer from significant high biases relative to the two reference

493 dataset. This could be due to a combination of parameter and structural errors in addition to
494 errors in the reference data themselves. The three LDAS simulations differ most during the
495 spring and fall months. Comparison of the seasonally averaged ET fluxes show overestimations
496 during MAM in all three LDAS products over the Southeast and Lower Mississippi River basin.
497 During JJA, the differences between the two Noah model-based simulations are more prominent
498 over vegetated crop regions in the upper Midwest and irrigated areas along the Mississippi river.
499 GLDAS product shows underestimation in ET during the SON months, whereas the NLDAS-
500 forced Noah simulations show better agreement with both FLUXNET and MOD16 estimates
501 during this period.
502
503 The assimilation of surface soil moisture impacts the ET estimates, particularly during the spring
504 (MAM) and summer (JJA) months, which is when the expected impacts would be largest due to
505 increasing soil moisture stress, insolation, and vegetation fraction conditions. The assimilation of
506 LPRM retrievals demonstrates systematic, statistically significant but modest improvements in
507 ET estimates relative to the Noah model simulation without data assimilation. The assimilation
508 of NASA retrievals, on the other hand, provides mixed results, with improvements in a few
509 regions of the NLDAS-domain. Overall, the integration using the NASA soil moisture retrievals
510 indicates degradation of the open loop ET estimates. The results also indicate strong correlations
511 between the improvements/degradations of ET estimates and the changes in soil moisture fields
512 introduced by soil moisture assimilation. Finally, the analysis of the sensible heat flux estimates
513 indicates consistent trends in both surface energy partition terms (latent and sensible estimates).
514

Acknowledgements

We gratefully acknowledge the financial support from the NASA Earth Science Technology Office (ESTO) (Advanced Information System Technology program award AIST-08-077), the NASA Energy and Water Cycle Study (NEWS), the Air Force Weather Agency, and NOAA's Climate Program Office. The efforts of NLDAS participants in generating the surface forcing is greatly appreciated. Some of the data used in this effort were acquired as part of the activities of NASA's Science Mission Directorate, and are archived and distributed by the Goddard Earth Sciences (GES) Data and Information Services Center (DISC). Computing was supported by the resources at the NASA Center for Climate Simulation.

REFERENCES

Baldocchi, D., et al., 2001; FLUXNET: A new tool to study the temporal and spatial variability of ecosystem-scale carbon dioxide, water vapor, and energy flux densities, Bull. Am. Meteorol. Soc., 82(11), 2415–2434.

Barlage, M., F. Chen, M. Tewari, K. Ikeda, D. Gochis, J. Dudhia, R. Rasmussen, B. Livneh, M. Ek, and K. Mitchell, 2010: Noah land surface model modifications to improve snowpack prediction in the Colorado Rocky Mountains, J. Geophys. Res., 115, D22101, doi:10.1029/2009JD013470.

Bonan, G. B., K. W. Oleson, M. Vertenstein, S. Levis, X. Zeng, Y. Dai, R. E. Dickinson, Z-L. Yang, 2002: The land surface climatology of the community land model coupled to the NCAR community climate model, J. Clim., 15 (22), 3123-3149.

Boone, A., F. Habets, J. Noilhan, E. Blyth, D. Clark, P. Dirmeyer, Y. Gusev, I. Haddeland, R. Koster, D. Lohmann, S. Mahanama, K. Mitchell, O. Nasanova, G.-Y. Niu, A. Pitman, J. Polcher, A. B. Shmakin, K. Tanaka, B. van den Hurk, S. Verant, D. Verseghy, and P. Viterbo, 2004: The Rhône-aggregation land surface scheme intercomparison project: An overview. J. Climate, 17, 187-208, doi: 10.1175/1520-0442(2004)017<0187:TRLSSI>2.0.CO;2.

Bowling, L.C. and D.P. Lettenmaier, 2010: Modeling the effects of lakes and wetlands on the water balance of Arctic Environments, J. Hydromet., 11, 276-295, doi: 10.1175/2009JHM1084.1.

Cosgrove, B.A., D. Lohmann, K.E. Mitchell, P.R. Houser, E.F. Wood, J. Schaake, A. Robock, C. Marshall, J. Sheffield, L. Luo, Q. Duan, R.T. Pinker, J.D. Tarpley, R.W. Higgins, and J. Meng, 2003: Real-time and retrospective forcing in the North American Land Data

549 Assimilation System (NLDAS) project. J. Geophys. Res., 108(D22), 8842,
550 doi:10.1029/2002JD003118.
551 Crow, W.T. and E.F. Wood, 2003: The assimilation of remotely sensed soil brightness
552 temperature imagery into a land surface model using ensemble kalman filtering: A case
553 study based on ESTAR measurements during SGP97. Advances in Water Resources, 26,
554 137-149.
555 Dai, Y., X. Zeng, R.E. Dickinson, I. Baker, G.B. Bonan, M.G. Bosilovich, A.S. Denning, P.A.
556 Dirmeyer, P.R. Houser, G.-Y. Niu, K.W. Oleson, C.A. Schlosser and Z.-L. Yang, 2003:
557 The Common Land Model (CLM), Bull. Amer. Meteor. Soc., Vol. 84, No. 8, 1013-1024.
558 Daly, C., R.P. Neilson, and D.L. Phillips, 1994: A statistical-topographic model for mapping
559 climatological precipitation over mountainous terrain. J. Appl. Meteor., 33, 140-158, doi:
560 10.1175/1520-0450(1994)033<0140:ASTMFM>2.0.CO;2.
561 Dickinson, R. E., A. Henderson-Sellers, P. J. Kennedy, and M. F. Wilson, 1986: Biosphere–
562 atmosphere transfer scheme (BATS) for the NCAR Community Climate Model. Tech.
563 Note TN-275+STR, 69 pp.
564 Drusch, M., 2007: Initializing numerical weather prediction models with satellite derived surface
565 soil moisture: Data assimilation experiments with ECMWF's integrated forecast system
566 and the TMI soil moisture dataset. J. Geophys. Res., 112, D03102,
567 doi:10.1029/2006JD007478.
568 Dirmeyer, P. A., 2011: A history of the Global Soil Wetness Project (GSWP). J. Hydrometeor.,
569 (in press), doi: 10.1175/JHM-D-10-05010.1.

570 Dirmeyer, Paul A., A. J. Dolman, Nobuo Sato, 1999: The Pilot Phase of the Global Soil Wetness
571 Project. Bull. Amer. Meteor. Soc., 80, 851–878, doi: 10.1175/1520-
572 0477(1999)080<0851:TPPOTG>2.0.CO;2
573 Dirmeyer, Paul A., Xiang Gao, Mei Zhao, Zhichang Guo, Taikan Oki, Naota Hanasaki, 2006:
574 GSWP-2: Multimodel Analysis and Implications for Our Perception of the Land Surface.
575 Bull. Amer. Meteor. Soc., 87, 1381–1397, doi: 10.1175/BAMS-87-10-1381.
576 Ek, M. B., K. E. Mitchell, Y. Lin, E. Rogers, P. Grunmann, V. Koren, G. Gayno, and J. D.
577 Tarpley, (2003), Implementation of Noah land-surface model advances in the NCEP
578 operational mesoscale Eta model, J. Geophys. Res., 108(D22), 8851, doi:
579 10.1029/2002JD003296.
580 Guo, Z., P. A. Dirmeyer, X. Gao, and M. Zhao, 2007: Improving the quality of simulated soil
581 moisture with a multi-model ensemble approach. Quart. J. Roy. Meteor. Soc., 133, 731-
582 747.
583 Henderson-Sellers, A., A. J. Pitman, P. K. Love, P. Irannejad, and T. H. Chen, 1995: The Project
584 for Intercomparison of Land Surface Parameterization Schemes (PILPS): Phases 2 and 3.
585 Bull. Amer. Meteor. Soc., 76, 489–503.
586 Jambor, U., P.R. Houser, M. Rodell, et al., 2002: Remotely sensed forcing data and the Global
587 Land Data Assimilation System. IEEE International Geoscience and Remote Sensing
588 Symposium (IGARSS 2002)/24th Canadian Symposium on Remote Sensing, 24-28 Jun
589 2002, Toronto, Canada; Vols. I-VI, Proceedings – Remote Sensing: Integrating Our View
590 of the Planet, pp. 1405-1407.
591 Jiménez, C., et al., 2011; Global intercomparison of 12 land surface heat flux estimates, J.
592 Geophys. Res., 116, D02102, doi:10.1029/2010JD014545.

593 Jung, M., M. Reichstein, and A. Bondeau, 2009: Towards global empirical upscaling of
594 FLUXNET eddy covariance observations: validation of a model tree ensemble approach
595 using a biosphere model, Biogeosciences, 6, 2001-2013.
596 Jung, M., M. Reichstein, P. Ciais, S.I.Seneviratne, J. Sheffield, M.L. Goulden, G. Bonan, A.
597 Cescatti, J. Chen, R. de Jeu, A. Johnanes Dolman, W. Eugster, D. Gerten, D. Gianelle, N.
598 Gobron, J. Heinke, J. Kimball, B. E. Law, L. Montagnani, Q. Mu, B. Mueller, K. Oleson,
599 D. Papale, A.D. Richardson, O. Roupsard, S. Running, E. Tomelleri, N. Viovy, U.
600 Weber, C. Williams, E. Wood, S. Zaehle and K. Zhang, 2010: Recent decline in the
601 global land evaportranspiration trend due to limited moisture supply, Nature,
602 doi:10.1038/nature09396.
603 Kato, H., M. Rodell, F. Beyrich, H. Cleugh, E. van Gorsel, H. Liu, and T.P. Meyers, 2007:
604 Sensitivity of land surface simulations to model physics, land characteristics, and
605 forcings at four CEOP sites. J. Meteor. Soc. Japan, 85A, 187-204.
606 Koster, R. D., and P. C. D. Milly, 1997: The interplay between transpiration and runoff
607 formulations in land surface schemes used with atmospheric models. J. Climate, 10,
608 1578–1591.
609 Kovalskyy, V., G.M. Henebry, B. Adusei, M. Hansen, D.P. Roy, and D.M. Mocko, 2011:
610 Spatially explicit comparison and performance assessment of an event driven phenology
611 model coupled with VegET evapotranspiration model. To be submitted to J. Geophys.
612 Res.
613 Kumar, S. V., C. D. Peters-Lidard, Y. Tian, J. Geiger, P. R. Houser, S. Olden, L. Lighty, J. L.
614 Eastman, P. Dirmeyer, B. Doty, J. Adams, E. Wood and J. Sheffield, 2006: LIS - An

615 Interoperable Framework for High Resolution Land Surface Modeling, Environmental
616 Modeling and Software, 21, 1402-1415.
617 Kumar, S.V., R. H. Reichle, C. D. Peters-Lidard, R. Koster, X. Zhan, W. Crow, J. Eylander, and
618 P.R. Houser, 2008: A land surface data assimilation framework using the Land
619 Information System: Description and Applications, Advances in Water Resources, 31,
620 1419-1432, doi: 10.1016/j.advwatres.2008.01.013.
621 Kumar, S.V., R.H. Reichle, R.Koster, W.T. Crow, and C.D. Peters-Lidard, 2009: Role of
622 subsurface physics in the assimilation of surface soil moisture observations, Journal of
623 Hydrometeorology, doi:10.1175/2009JHM1134.1.
624 Lawrence, D.M., K.W. Oleson, M.G. Flanner, P.E. Thornton, S.C. Swenson, P.J. Lawrence, X.
625 Zeng, Z.-L. Yang, S. Levis, K. Sakaguchi, G.B. Bonan, and A.G. Slater, 2011:
626 Parameterization improvements and functional and structural advances in version 4 of the
627 Community Land Model. J. Adv. Model. Earth Sys., 3, DOI: 10.1029/2011MS000045.
628 Livneh, B., Y. Xia, K. E. Mitchell, M. B. Ek, and D. P. Lettenmaier, 2010: Noah LSM Snow
629 Model Diagnostics and Enhancements, J. Hydromet., 11, 721-738.
630 Liang, X., E. F. Wood, and D. Lettenmaier, Surface and soil moisture parameterization of the
631 VIC-2L model: Evaluation and modifications, 1996: Global Planet. Change, 13, 195-206.
632 Liu, Q., R.H. Reichle, R. Bindlish, M.H. Cosh, W.T. Crow, R. de Jeu, G.J.M. De Lannoy, G.J.
633 Huffman, T.J. Jackson, 2011: The contributions of precipitation and soil moisture
634 observations to the skill of soil moisture estimates in a land data assimilation system,
635 Journal of Hydrometeorology, doi:10.1175/JHM-D-10.05000.
636 Livneh, B, Y. Xia, K.E. Mitchell, M.B. Ek, and D. Lettenmaier, 2010: Noah LSM snow model
637 diagnostics and enhancements. J. Hydrometeor., 11, 721–738.

638 Lohmann, D., K.E. Mitchell, P.R. Houser, E.F. Wood, J.C. Schaake, A. Robock, B.A. Cosgrove,
639 J. Sheffield, Q. Duan, L. Luo, W. Higgins, R.T. Pinker, and J.D. Tarpley, 2004:
640 Streamflow and water balance intercomparisons of four land surface models in the North
641 American Land Data Assimilation System project. J. Geophys. Res., 109, D07S91,
642 doi:10.1029/2003JD003517.
643 Luo, L., A. Robock, K.E. Mitchell, P.R. Houser, E.F. Wood, J.C. Schaake, D. Lohmann, B.A.
644 Cosgrove, F. Wen, J. Sheffield, Q. Duan, R.W. Higgins, R.T. Pinker, and J.D. Tarpley,
645 2003: Validation of the North American Land Data Assimilation System (NLDAS)
646 retrospective forcing over the southern Great Plains. J. Geophys. Res., 108(D22), 8843,
647 doi:10.1029/2002JD003246.
648 Manabe, S., 1969: Climate and the circulation. I. The atmospheric circulation and the hydrology
649 of the earth's surface. Mon. Wea. Rev., 97, 739–774.
650 Mesinger, F., G. DiMego, E. Kalnay, K.E. Mitchell, P.C. Shafran, W. Ebisuzaki, D. Jovic, J.
651 Woollen, E. Rogers, E.H. Berbery, M.B. Ek, Y. Fan, R. Grumbine, W. Higgins, H. Li, Y.
652 Lin, G. Manikin, D. Parrish, and W. Shi., 2006: North American Regional Reanalysis.
653 Bull. Amer. Meteor. Soc., 87, 343-360.
654 Mitchell, K.E., D. Lohmann, P.R. Houser, E.F. Wood, J.C. Schaake, A. Robock, B.A. Cosgrove,
655 J. Sheffield, Q. Duan, L. Luo, R.W. Higgins, R.T. Pinker, J.D. Tarpley, D.P. Lettenmaier,
656 C.H. Marshall, J.K. Entin, M. Pan, W. Shi, V. Koren, J. Meng, B. H. Ramsay, and A.A.
657 Bailey, 2004: The multi-institution North American Land Data Assimilation System
658 (NLDAS): Utilizing multiple GCIP products and partners in a continental distributed
659 hydrological modeling system. J. Geophys. Res., 109, D07S90,
660 doi:10.1029/2003JD003823.

661 Mo, K.C., L.N. Long, Y. Xia, S.K. Yang, J.E. Schemm, and M. Ek, 2011: Drought Indices Based
662 on the Climate Forecast System Reanalysis and Ensemble NLDAS. J. Hydrometeor.,
663 12(2), 181-205, doi:10.1175/2010JHM1310.1.
664 Mu, Q., F.A. Heinsch, M. Zhao, and S. Running, 2007: Development of a global
665 evapotranspiration algorithm based on MODIS and global meteorology data, Remote
666 Sensing of Environment, 111(4), 519-536.
667 Mu, Q., M. Zhao, S.W. Running, 2011: Improvements to a MODIS Global Terrestrial
668 Evapotranspiration Algorithm, Remote Sensing of Environment, in press.
669 Mueller, B., et al., 2011: Evaluation of global observations-based evapotranspiration datasets
670 and IPCC AR4 simulations, Geophys. Res. Lett., 38, L06402,
671 doi:10.1029/2010GL046230.
672 National Research Council, 2011: Global Change and Extreme Hydrology: Testing Conventional
673 Wisdom. Washington, DC: National Academies Press, 60pp.
674 National Research Council, 2010: Assessment of Intraseasonal to Interannual Climate Prediction
675 and Predictability. Washington, DC: National Academies Press, 192pp.
676 Njoku, E.G., T.L. Jackson, V. Lakshmi, T.Chan, and S.V. Nghiem, 2003: Soil moisture retrieval
677 from AMSR-E, IEEE Transactions on Geoscience and Remote Sensing, 41 (2): 215-229.
678 Owe, M., R.A.M. de Jeu, and T.R. H. Holmes, 2008: Multi-sensor historical climatology of
679 satellite-derived global land surface moisture, J. Geophys. Res. 13, F01002,
680 doi:1029/2007JF000769.
681 Pan, M., P. Ming, J. Sheffield, E.F. Wood, K.E. Mitchell, P.R. Houser, J.C. Schaake, A. Robock,
682 D. Lohmann, B. Cosgrove, Q. Duan, L. Luo, R.W. Higgins, R.T. Pinker, and J.D.
683 Tarpley, 2003: Snow process modeling in the North American Land Data Assimilation

684 System (NLDAS): 2. Evaluation of model simulated snow water equivalent. J. Geophys.
685 Res., 108(D22), 8850, doi:10.1029/2003JD003994.
686 Peters-Lidard, C.D., P.R. Houser, Y. Tian, S.V. Kumar, J.V. Geiger, S. Olden, L. Lighty, J.L.
687 Eastman, B. Doty, P. Dirmeyer, J. Adams, K. Mitchell, E.F. Wood, and J. Sheffield,
688 2007: High-performance earth system modeling with NASA/GSFC's Land Information
689 System, Innovations in Systems and Software Engineering, 3(3), 157-165.
690 Pitman, A. J., and A. Henderson-Sellers, 1998: Recent progress and results from the Project for
691 the Intercomparison of Landsurface Parameterizations Schemes. J. Hydrol., 212–213,
692 128–135.
693 Reichle, R.H., D. M. McLaughlin, and D.A. Entekhabi, 2002: Hydrologic data assimilation with
694 the ensemble Kalman filter, Monthly Weather Review, 130, 1, 103-114.
695 Reichle, R.H. and R Koster, 2004: Bias reduction in short records of satellite soil moisture,
696 Geophys. Res. Lett. L19501,doi:10.1029/2004GL020938.
697 Reichle, R.H., R.D. Koster, P. Liu, S.P.P. Mahanama, E.G. Njoku, and M. Owe, 2007:
698 Comparison and assimilation of global soil moisture retrievals from the Advanced
699 Microwave Scanning Radiometer for the Earth Observing System (AMSR-E) and the
700 Scanning Multichannel Microwave Radiometer (SMMR), J. Geophys. Res., 112,
701 D09108, doi:10.1029/2006JD008033.
702 Robock, A., L. Luo, E.F. Wood, F. Wen, K.E. Mitchell, P.R. Houser, J.C. Schaake, D. Lohmann,
703 B. Cosgrove, J. Sheffield, Q. Duan, R.W. Higgins, R.T. Pinker, J.D. Tarpley, J.B. Basara,
704 and K.C. Crawford, 2003: Evaluation of the North American Land Data Assimilation
705 System over the southern Great Plains during the warm season. J. Geophys. Res.,
706 108(D22), 8846, doi:10.1029/2002JD003245.

Rodell, M., P.R. Houser, U. Jambor, J. Gottschalck, K. Mitchell, C.-J. Meng, K. Arsenault, B. Cosgrove, J. Radakovich, M. Bosilovich, J.K. Entin, J.P. Walker, D. Lohmann, and D. Toll, 2004a The Global Land Data Assimilation System. Bull. Amer. Meteor. Soc., 85(3), 381-394.

Rodell, M., J.S. Famiglietti, J. Chen, S. Seneviratne, P. Viterbo, S. Holl, and C. R. Wilson, 2004b: Basin scale estimates of evapotranspiration using GRACE and other observations. Geophys. Res. Lett., 31, L20504, doi:10.1029/2004GL020873.

Rodell, M., and P.R. Houser, Updating a land surface model with MODIS derived snow cover, 2004, J. Hydromet., 5(6), 1064-1075.

Schaake, J.C., Q. Duan, V. Koren, K.E. Mitchell, P.R. Houser, E.F. Wood, A. Robock, D.P. Lettenmaier, D. Lohmann, B.A. Cosgrove, J. Sheffield, L. Luo, R.W. Higgins, R.T. Pinker, and J.D. Tarpley, 2004: An intercomparison of soil moisture fields in the North American Land Data Assimilation System (NLDAS). J. Geophys. Res., 109, D01S90, doi:10.1029/2002JD003309.

Sellers, P. J., Y. Mintz, Y. C. Sud, and A. Dalcher, 1986: A simple biosphere model (SiB) for use within general circulation models. J. Atmos. Sci., 43, 505–531.

Sheffield, J., M. Pan, E.F. Wood, K.E. Mitchell, P.R. Houser, J.C. Schaake, A. Robock, D. Lohmann, B. Cosgrove, Q. Duan, L. Luo, R.W. Higgins, R.T. Pinker, J. Dan Tarpley, and B.H. Ramsay, 2003: Snow process modeling in the North American Land Data Assimilation System (NLDAS): 1. Evaluation of model-simulated snow cover extent. J. Geophys. Res., 108(D22), 8849, doi:10.1029/2002JD003274.

728 Syed, T.H., J.S. Famiglietti, M. Rodell, J.L. Chen, and C.R. Wilson, 2008: Analysis of terrestrial
729 water storage changes from GRACE and GLDAS. Water Resour. Res., 44, W02433,
730 doi:10.1029/2006WR005779.
731 Troy, T.J., E.F. Wood, and J. Sheffield, 2008: An efficient calibration method for continental-
732 scale land surface modeling. Water Resour. Res., 44, W09411,
733 doi:10.1029/2007WR006513.
734 Wei, H., Y. Xia, K.E. Mitchell, and M.B. Ek, 2011: Improvement of the Noah Land Surface
735 Model for Warm Season Processes: Evaluation of Water and Energy Flux Simulation.
736 To be submitted to Geophys. Res. Letters.
737 Xia, Y., K. Mitchell, M. Ek, J. Sheffield, E.F. Wood, B. Cosgrove, L. Luo, C. Alonge, H. Wei, J.
738 Meng, B. Livneh, D. Lettenmaier, V. Koren, Y. Duan, K. Mo, and Y. Fan, 2011a:
739 Continental-Scale Water and Energy Flux Analysis and Validation for the North-
740 American Land Data Assimilation System Project Phase 2 (NLDAS-2), Part 1:
741 Comparison Analysis and Application of Model Products. To be submitted to J.
742 Geophys. Res.
743 Xia, Y., K. Mitchell, M. Ek, J. Sheffield, B. Cosgrove, L. Luo, C. Alonge, H. Wei, J. Meng, B.
744 Livneh, Y. Duan, and D. Lohmann, 2011b: Continental-Scale Water and Energy Flux
745 Analysis and Validation for the North-American Land Data Assimilation System Project
746 Phase 2 (NLDAS-2), Part 2: Validation of Model-Simulated Streamflow. To be
747 submitted to J. Geophys. Res.
748 Xia, Y., M. Ek, H. Wei, and J. Meng, 2011c: Comparative Analysis of Relationships between
749 NLDAS-2 Forcings and Model Outputs. Submitted to Hydrological Processes.
750

751 **List of Tables**

752

762

763

Table 1: Parameters for perturbations to meteorological forcings and soil moisture prognostic model variables in the data assimilation integrations.

Variable	Perturbation Type	Standard Deviation	Cross Correlations with perturbations in			
Meteorological Forcings						
			Downward Shortwave	Downward Longwave	Precipitation	
Downward Shortwave	Multiplicative	0.3 [-]	1.0	-0.5	-0.8	
Downward Longwave	Additive	50 Wm^{-2}	-0.5	1.0	0.5	
Precipitation	Multiplicative	0.5 [-]	-0.8	0.5	1.0	
Noah LSM soil moisture states						
			Sm1	Sm2	Sm3	Sm4
Total soil moisture – layer 1 (sm1)	Additive	0.6E-3 m^3m^{-3}	1.0	0.6	0.4	0.2
Total soil moisture – layer 2 (sm2)	Additive	1.1E-4 m^3m^{-3}	0.6	1.0	0.6	0.4
Total soil moisture – layer 3 (sm3)	Additive	0.6E-5 m^3m^{-3}	0.4	0.6	1.0	0.6
Total soil moisture – layer 4 (sm4)	Additive	0.4E-5 m^3m^{-3}	0.2	0.4	0.6	1.0

Table 2: NLDAS domain-averaged root mean square and bias errors (all with 95% confidence intervals) in latent heat flux (Qle) and sensible heat flux (Qh) estimates from five LDAS simulations with respect to two reference datasets : (1) the gridded FLUXNET data from Jung et al., (2009) and (2) MOD16 data from Mu et al. (2011), which only provides Qle. Two of the NLDAS simulations show differences due to Noah version, and two of the NLDAS simulations include soil moisture data assimilation from the NASA and LPRM products, as discussed in the text.

	FLUXNET		**MOD16**	
Qle	**RMSE (Wm^{-2})**	**Bias (Wm^{-2})**	**RMSE (Wm^{-2})**	**Bias (Wm^{-2})**
GLDAS	24.7 ± 0.3	5.5 ± 0.4	28.0 ± 0.2	4.4 ± 0.3
NLDAS (Noah v2.7.1)	19.3 ± 0.3	11.9 ± 0.4	21.5 ± 0.2	10.3 ± 0.3
NLDAS (Noah v3.2)	27.6 ± 0.3	12.9 ± 0.4	22.7 ± 0.2	11.2 ± 0.3
NLDAS (Noah v3.2)+NASA DA	29.4 ± 0.3	15.9 ± 0.4	24.5 ± 0.2	14.2 ± 0.3
NLDAS (Noah v3.2)+LPRM DA	25.6 ± 0.3	10.9 ± 0.3	21.9 ± 0.2	9.2 ± 0.3
Qh				
GLDAS	23.4 ± 0.2	-5.6 ± 0.4	N/A	N/A
NLDAS (Noah v2.7.1)	21.1 ± 0.3	-7.0 ± 0.4	N/A	N/A
NLDAS (Noah v3.2)	32.5 ± 0.3	-9.2 ± 0.4	N/A	N/A
NLDAS (Noah v3.2)+NASA DA	34.5 ± 0.3	-12.2 ± 0.4	N/A	N/A
NLDAS (Noah v3.2)+LPRM DA	30.4 ± 0.3	-7.3 ± 0.4	N/A	N/A

List of Figures

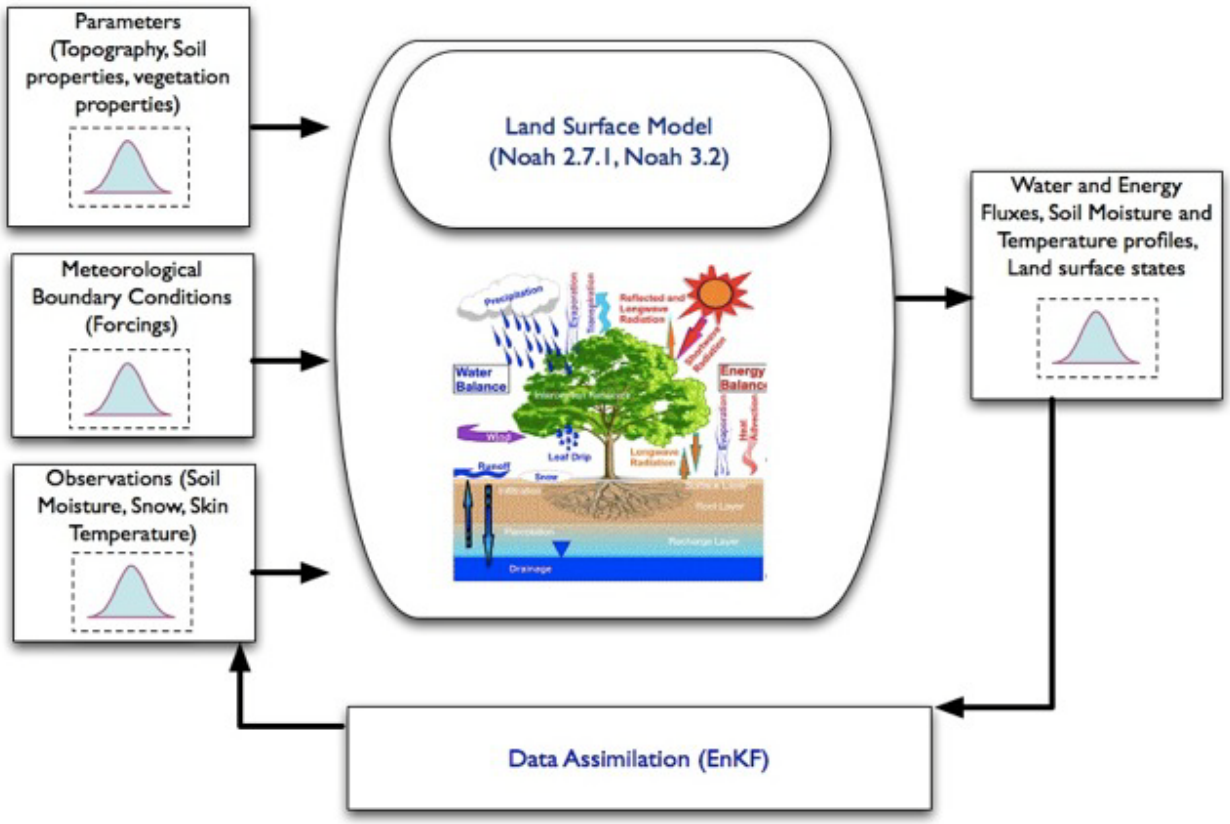

Figure 1: Schematic illustrating the data flows in an uncoupled Land Data Assimilation System. As shown, input parameter and meteorological data or "forcings" can obtained from various sources. If data assimilation is employed, the observations of land surface states can be used to update model states using various data assimilation approaches, such as Direct Insertion (DI) or Ensemble Kalman Filter (EnKF).

823

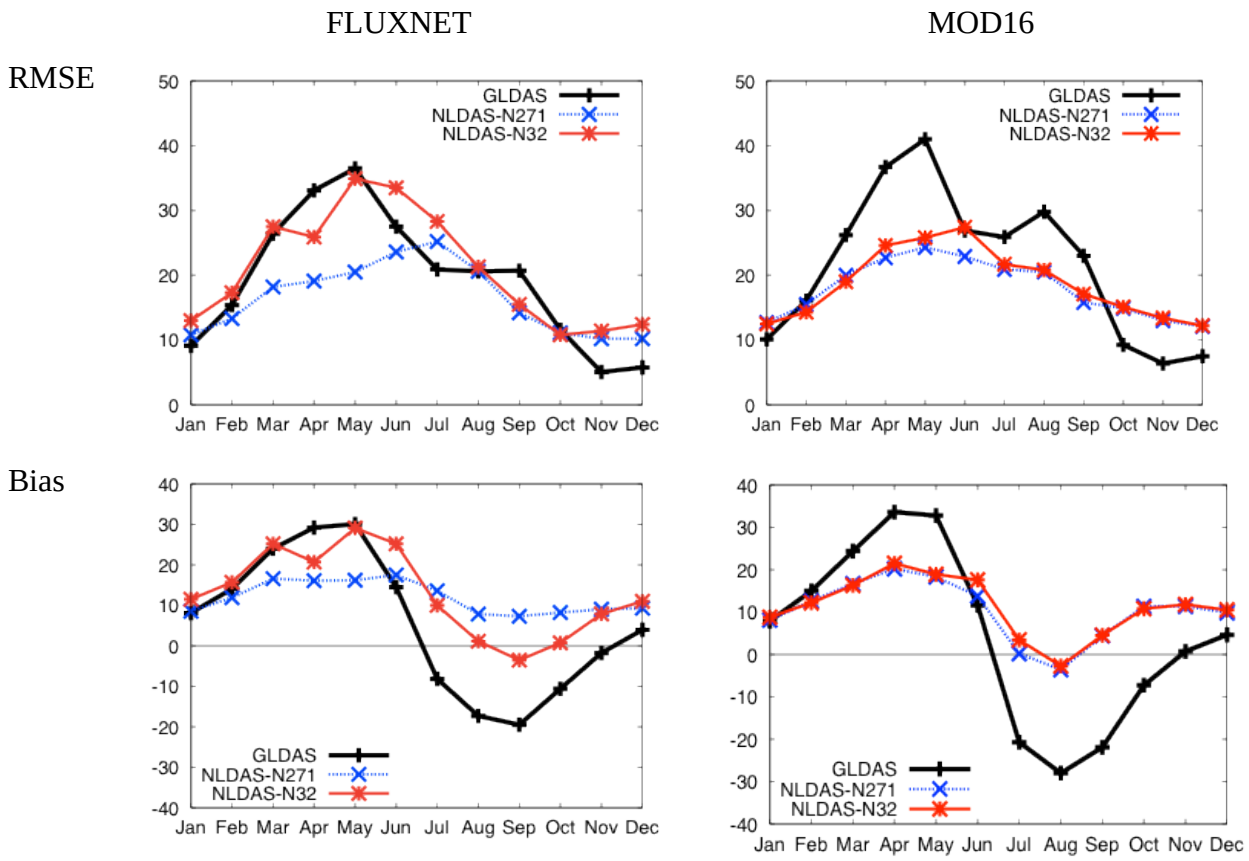

824 **Figure** 2**: Comparison of the average seasonal cycles of RMSE and Bias for latent heat flux**
825 **(Qle) estimates from the three LDAS simulations: GLDAS Noah, NLDAS-like simulations**
826 **with Noah 2.7.1 (NLDAS-N271) and Noah 3.2 (NLDAS-N32) compared against the gridded**
827 **FLUXNET data (left column) and MOD16 data (right column). All units are in Wm^{-2}.**

828

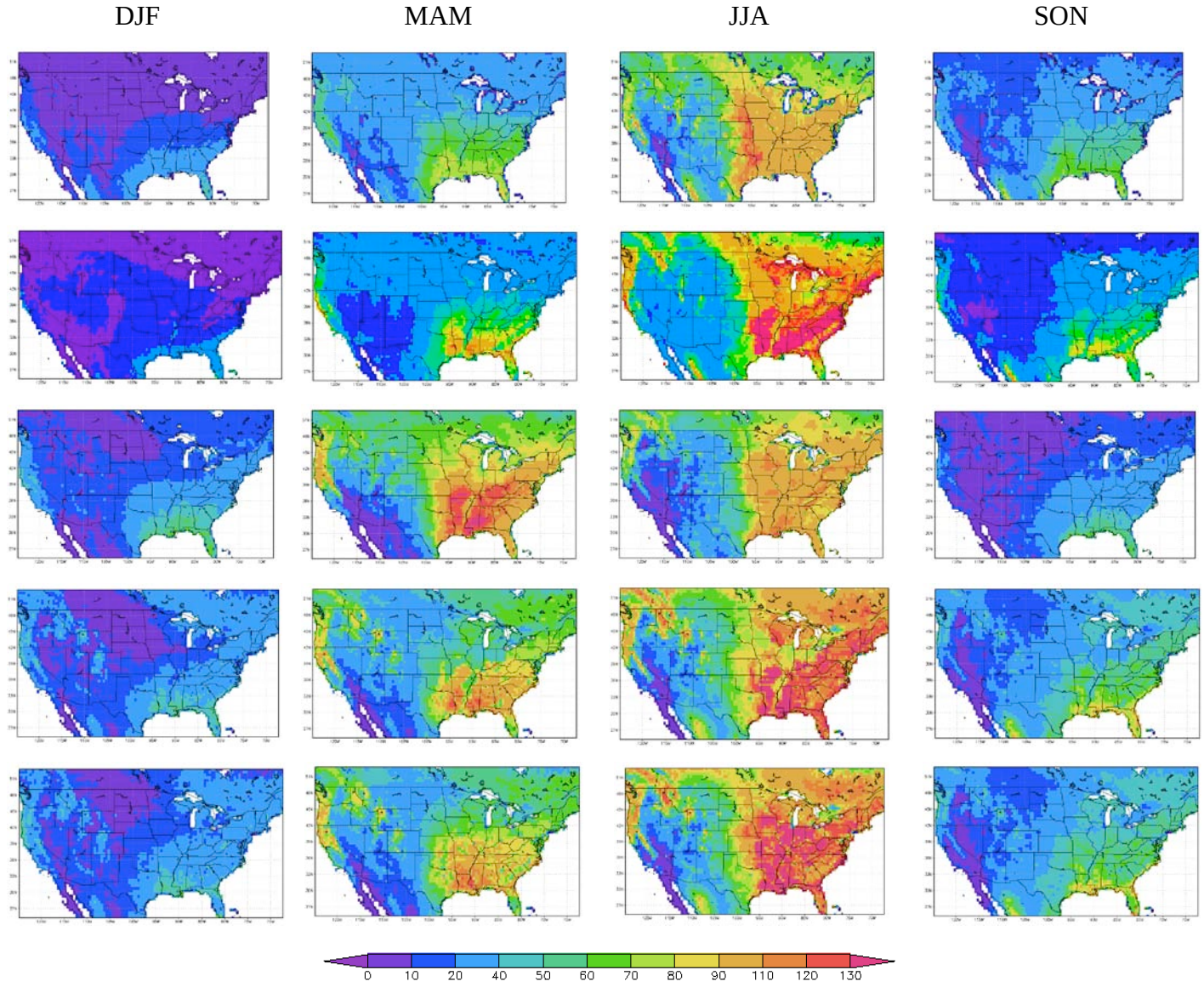

829

830 **Figure 3:Intercomparison of seasonally-averaged Qle for the period Jan 2002-Dec 2008 over the NLDAS domain from five sources: gridded**
831 **FLUXNET (Jung et al., 2010); MOD16 data (Mu et al. 2011); GLDAS Noah (Rodell et al., 2004); NLDAS-like simulations with Noah 2.7.1**
832 **and Noah3.2 produced using LIS (Kumar et al., 2006). All units are in Wm^{-2}.**

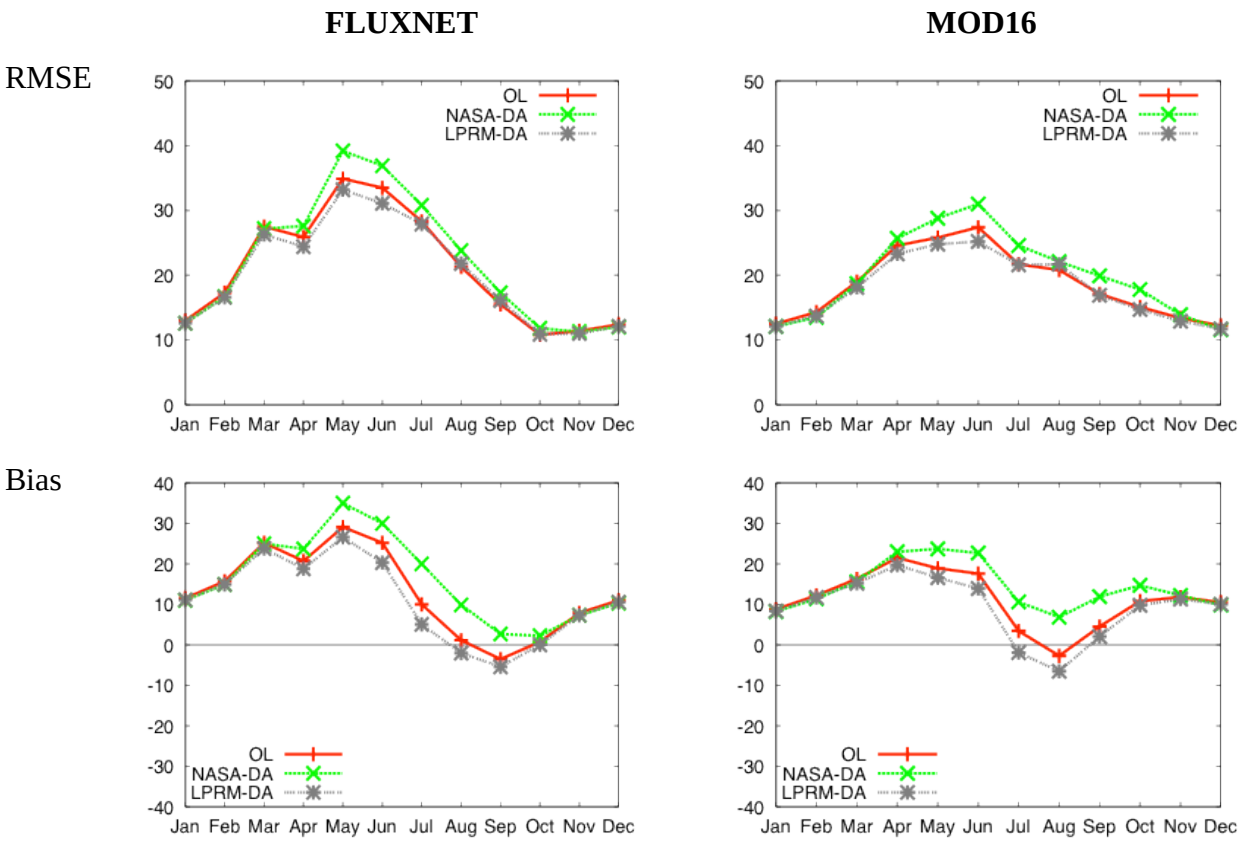

Figure 4: Comparison of the seasonal cycles of RMSE and Bias in Qle estimates from NLDAS-equivalent simulations for the period Jan 2002- Dec 2008 against the gridded FLUXNET data (left column) and MOD16 data (right column). The comparisons present the impact of the assimilation of surface soil moisture retrievals on latent heat flux estimates. OL represents the "open loop" model simulation without data assimilation, which is equivalent to the NLDAS-N32 curves in Figure 2. NASA-DA and LPRM-DA represents simulations that assimilate the NASA and LPRM retrievals of AMSR-E soil moisture, respectively. All units are in Wm^{-2}.

845

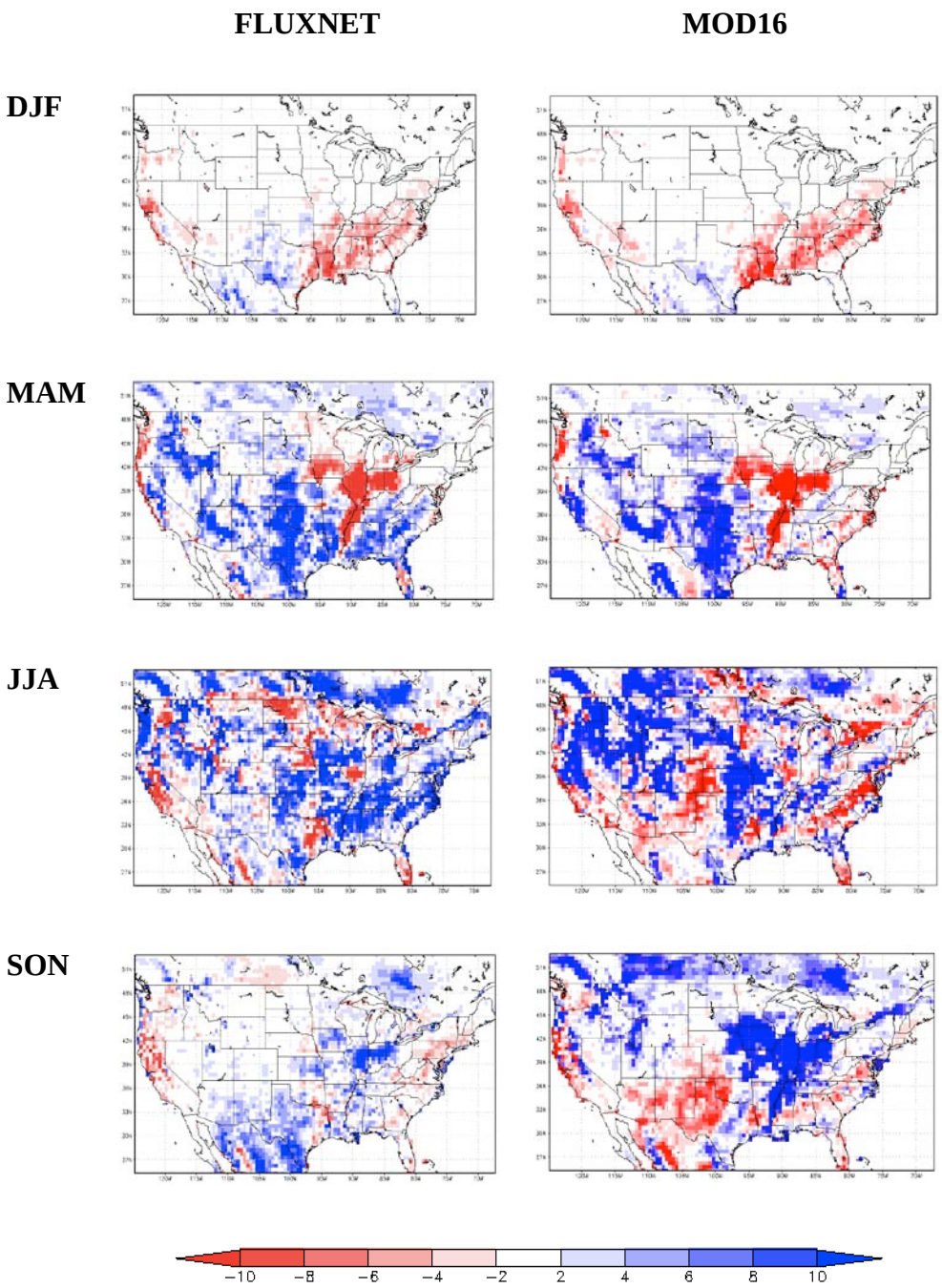

846 **Figure 5: Comparison of the latent heat flux improvement metric (RMSE (DA) – RMSE**
847 **(OL)) from the data assimilation integrations using the NASA AMSR-E soil moisture**
848 **retrievals (NASA-DA). The two columns represent the reference datasets used in the**
849 **RMSE computations: FLUXNET (left column) and MOD16 (right column). The red and**

blue shades indicate improvements and degradations as a result of data assimilation, respectively. All units are in Wm^{-2}.

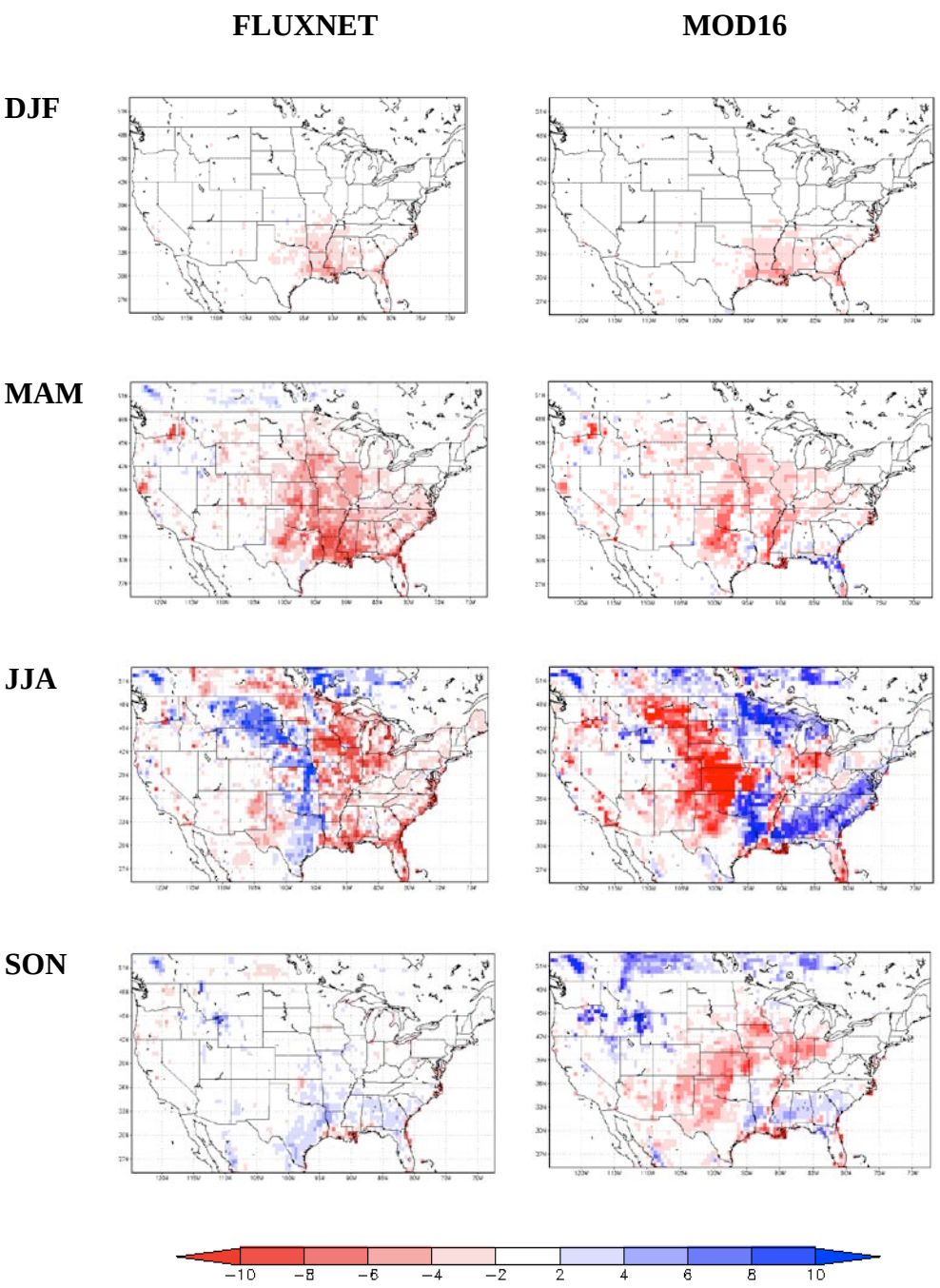

Figure 6: Same as Figure 5, but from data assimilation integrations using LPRM AMSR-E soil moisture retrievals (LPRM-DA).

858
859

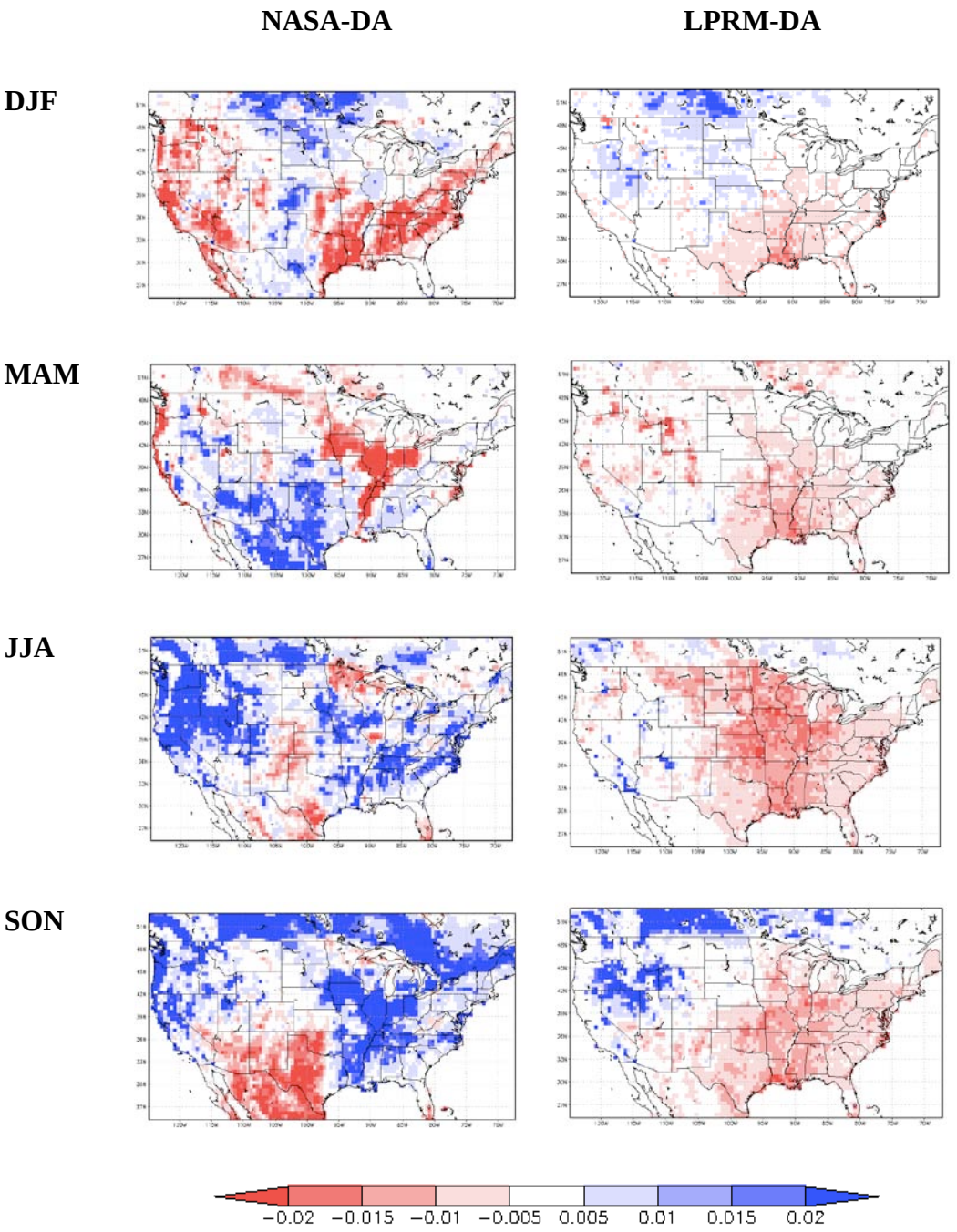

860 **Figure 7: Comparison of the mean soil moisture difference maps (soil moisture (DA) – soil**
861 **moisture (OL)) from soil moisture data assimilation integrations. The left and right panels**
862 **represent the NASA-DA and LPRM-DA, respectively. All units are in m^3m^{-3}.**